Mechanisms of Double Resonance in Solids

J. LAMBE, N. LAURANCE, E. C. MCIRVINE, AND R. W. TERHUNE
Scientific Laboratory, Ford Motor Company, Dearborn, Michigan
(Received November 10, 1960)

A study of electron-nuclear double resonance (ENDOR) in ruby and other solids demonstrates the existence of the "distant-ENDOR" effect, which involves a change in the electron paramagnetic resonance (EPR) signal caused by the depolarization of "distant" nuclei (nuclei having negligible hyperfine interaction with the paramagnetic centers). In order to obtain interpretable data on the mechanism, it proved necessary to perform most of the experiments without modulation, observing not the derivatives but the functions χ' and χ'' themselves, the dispersive and absorptive parts of the spin susceptibility. The former shows a large decrease upon application of rf power at a nuclear transition frequency; the latter shows a moderate increase. Both the distant ENDOR (Al^{27} nuclear Zeeman frequencies) and local ENDOR (Cr^{53} hyperfine frequencies) affect the EPR with a response time comparable to the spin-lattice relaxation time of the distant aluminum nuclei. Nuclear-nuclear double-resonance experiments show that applied rf corresponding to Cr^{53} nuclear transitions depolarizes Al^{27} nuclei. Both of these observations are consistent with a mechanism involving dynamic nuclear polarization. A theoretical analysis of this mechanism, based on forbidden transitions involving distant nuclei, gives good agreement with observed nuclear polarizations and with the observed behavior of χ', but predicts small increases in χ''. The increased absorption signal may be explained by enhanced spectral spin diffusion or by a spin packet considerably wider than assumed. Distant ENDOR is expected to occur quite generally.

I. INTRODUCTION

THE technique of electron-nuclear double resonance (ENDOR) developed by Feher[1–5] has proved an important method for the study of hyperfine interactions in solids. By observing changes in an electron paramagnetic resonance (EPR) signal, one determines a radio-frequency spectrum corresponding to nuclear magnetic resonance (NMR) transitions. In effect, it is possible to make NMR measurements with greatly enhanced sensitivity.

The mechanisms which lead to ENDOR effects are of considerable interest for the understanding of electron-nuclear interactions in solids. Recently we have made ENDOR measurements[6] on materials in which the ENDOR mechanism appears different from that operative in the systems studied by Feher. Dynamic nuclear polarization[7,8] appears to be intimately related to ENDOR behavior in our systems. In this paper we report a more detailed study of these cases.

In discussing ENDOR it is important to distinguish between effects which occur in absorption and dispersion. By "absorption ENDOR effects" are meant changes in the absorptive part of the electron spin susceptibility caused by the stimulation of NMR transitions by applied rf. "Dispersion ENDOR effects" similarly means changes in the dispersive part of the electron spin susceptibility due to the same cause. In the case of homogeneously-broadened lines with resolved hyperfine splitting, dispersion and absorption ENDOR effects go hand in hand, increasing and decreasing proportionately. Inhomogeneously-broadened lines, on the other hand, can show various pure or mixed ENDOR responses. For example, a pure absorption ENDOR effect would occur if the application of the NMR signal simply changed the degree of saturation of the spin packet at the applied microwave frequency. A pure dispersion ENDOR effect could result from an assymetric "skewing" of the line-shape with no change in total absorption.

Feher proposed a model[4] which satisfactorily accounted for the results of his ENDOR experiments. Consider an inhomogeneously-broadened EPR line. This line, of width $1/T_2^*$ cps, is composed of a group of "spin packets" of natural width $1/T_2$ cps. The spectral position of a spin packet within the line is determined by the orientation of the nearby nuclei. If one examines the electron paramagnetic resonance at a fixed magnetic field at high microwave power, one saturates a group of packets whose resonant frequency corresponds to the applied microwave frequency. As saturation proceeds, the EPR absorption signal decreases. Now, however, one can apply a radio-frequency field which flips nearby nuclei, shifting other, unsaturated electron-spin packets so that these packets become resonant with the microwave field and can absorb energy. The EPR absorption signal should then increase.

Since Feher made use of magnetic-field modulation and fast-passage techniques, the remainder of his analysis deals with these complications. The basic mechanism is, however, described above.

Recently, ENDOR experiments on ruby were reported[6] in which the mechanism could not be understood in terms of this model alone. The salient features of the observation were: (1) A large *decrease* in the EPR signal occurred upon application of a radio-frequency field corresponding to nuclear transitions whereas, as we have indicated above, the absorption signal is expected to increase. (2) The recovery time of the signal upon re-

[1] G. Feher, Phys. Rev. **103**, 500 (1956).
[2] G. Feher and E. A. Gere, Phys. Rev. **103**, 501 (1956).
[3] G. Feher, Phys. Rev. **103**, 834 (1956).
[4] G. Feher, Phys. Rev. **114**, 1219 (1959).
[5] G. Feher and E. A. Gere, Phys. Rev. **114**, 1245 (1959).
[6] R. W. Terhune, J. Lambe, G. Makhov, and L. G. Cross, Phys. Rev. Letters **4**, 234 (1960).
[7] A. Abragam and W. G. Proctor, Compt. rend. **246**, 2253 (1958).
[8] M. Abraham, M. A. H. McCausland, and F. N. H. Robinson, Phys. Rev. Letters **2**, 449 (1959).

moval of the nuclear transition frequency was comparable with the nuclear spin-lattice relaxation time, whereas the above model predicts a recovery time comparable with the electron spin-lattice relaxation time. (3) The effect was observed at frequencies which flip "distant" aluminum nuclei as well as frequencies which flip the nucleus of the paramagnetic chromium ion itself. By distant nuclei in ruby, we mean aluminum nuclei sufficiently removed from the paramagnetic center that their resonance shows no detectable shift due to the presence of the paramagnetic ion. Clearly, the flipping of such nuclei does not significantly alter the spectral position of a spin packet, and thus no ENDOR effect is predicted on the above model. The effect which involves distant nuclei we will term "distant ENDOR." The effect involving nuclei having large hyperfine interaction with the electron spin system we will term "local ENDOR."

The present work was undertaken to clarify the mechanisms involved in the ENDOR effect. In the course of this work it was recognized that a careful distinction must be made between χ' and χ'', the dispersive and absorptive components of the electron paramagnetic susceptibility. The most straightforward method for doing this experimentally is to dispense with the usual magnetic field modulation. For this reason, the EPR results reported here were obtained without magnetic field modulation. It will be shown that in the present ENDOR experiments χ' decreases while χ'' increases upon application of the nuclear transition frequencies. Thus it will be seen that in discussing the mechanism of ENDOR, the term "EPR signal" is not sufficiently definitive.

As a result of this study, we propose that the ENDOR behavior in ruby depends upon the existence of induced nuclear polarization. Such polarization has been observed in a number of solid materials,[7,8] including ruby.[9] Dynamic nuclear polarization appears to be a quite general phenomenon, and wherever it exists its presence should affect ENDOR behavior. The mechanisms discussed here must not be construed to supercede that proposed by Feher; rather, they apply under a different set of circumstances. In particular, a relatively high concentration of paramagnetic impurities is probably necessary in order to make the nuclear spin-lattice relaxation time reasonable for the observation of ENDOR effects which involve nuclear polarization.

The details of the ENDOR hyperfine spectrum of ruby have been studied and will be published separately.[10] In the present work we shall be concerned only with the ENDOR mechanism and will ignore the details of the ruby spectrum. A possible mechanism of distant ENDOR is discussed which intrinsically involves forbidden transitions and dynamic nuclear polarization by the Abragam scheme.[7]

Two important operational aspects of double resonance are established in this paper. Firstly, the ENDOR technique can be applied to *distant* nuclei in many materials. Secondly, double-nuclear resonance can be performed in materials where one of the nuclear species is present in very dilute amounts. In addition, the double-nuclear resonance can be performed with enhanced sensitivity if the population of "detector-nuclei" is originally dynamically polarized through the application of microwave power to the paramagnetic impurities. These two technical observations should allow double-resonance techniques to be applied to the hyperfine spectroscopy of many nuclei unapproachable by NMR techniques.

II. EXPERIMENTAL PROCEDURE

All the quantitative measurements reported here were made on pink ruby (Al_2O_3: Cr^{3+}) with chromium ion concentrations of 0.1%. These crystals were obtained from the Linde Company. They were cut into rectangular parallelopipeds with the c axis of the crystal parallel to one of the short edges of the sample. A typical sample measured 3 mm×3 mm×15 mm. Measurements performed on other materials, such as dilute ruby (lower chromium ion concentrations) and GASH, will be discussed only qualitatively.

For ENDOR measurements, the sample was inserted

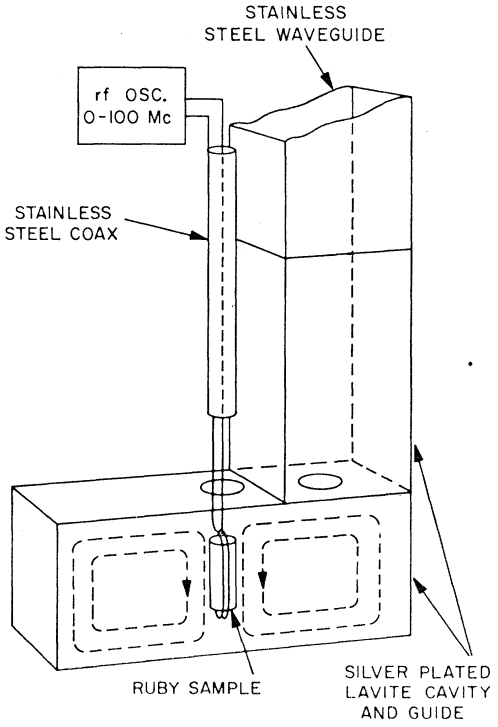

FIG. 1. Apparatus used in making electron-nuclear double resonance measurements.

[9] J. A. Cowen, W. R. Schafer, and R. D. Spence, Phys. Rev. Letters **3**, 13 (1959).

[10] R. W. Terhune, J. Baker, C. Kikuchi, and J. Lambe (to be published). See also C. Kikuchi, J. Lambe, G. Makhov, and R. W. Terhune, J. Appl. Phys. **30**, 1061 (1959), for detailed references.

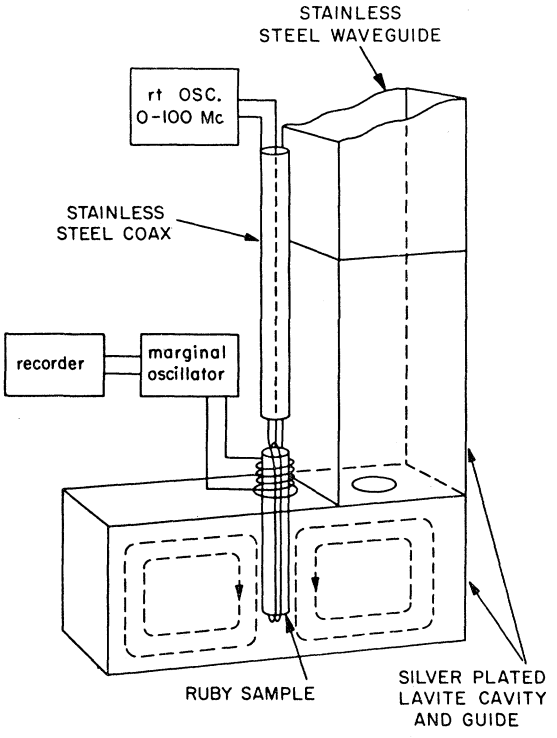

FIG. 2. Apparatus used to make simultaneous measurements of electron paramagnetic resonance and nuclear magnetic resonance while an auxiliary radio-frequency coil induces nuclear transitions.

into a lavite cavity which has been described previously.[11] The cavity (Fig. 1) had a fixed coupling iris and a hole at the top for introducing the sample. All experiments were performed at 4.2°K with the cavity immersed in liquid helium. The ruby sample was mounted on a Lucite holder fastened to a long stainless-steel tube. Two turns of fine copper wire encircled the sample, and the tube served as the shield of a coaxial lead to this coil. The sample was mounted so that the c axis of the ruby was parallel to the plane of the coil.

The microwave spectrometer was of conventional design. Magnetic field was supplied by a Varian 12-in. magnet with a $5\frac{1}{4}$-in. gap. The microwave source was a Laboratory for Electronics X-band generator which was tuned to match the resonant frequency of the cavity. The source was frequency-stabilized either with reference to auxiliary cavities within the source or with reference to the sample cavity. The latter mode of operation had to be used to observe the absorption component of the susceptibility, especially at high power levels.

An important part of the spectrometer is the microwave circulator, which transmits microwave power to the sample and transmits the reflected signal to a crystal detector. A bypass arm with variable amplitude and phase is used to bias the crystal so that it operates in its most sensitive region. For detection of very small signals, a superheterodyne operation was employed with an i.f. of 30 Mc/sec.

Since it was desired to observe directly the signal, and not its derivative, no magnetic-field modulation was used in the measurements on 0.1% ruby. The signal from the crystal detector was amplified by a dc amplifier and directly applied to the y axis of an x-y recorder. The x axis of this recorder was driven by the magnet current so that the traces are linear in field.

Subsequent modifications of the apparatus were made to permit observation of the Al^{27} NMR signal in the ruby specimen while performing the ENDOR experiment. For these measurements, magnetic-field modulation at 90 cps was used and the NMR signal was observed with a conventional marginal oscillator. The modified crystal holder is shown in Fig. 2. An additional coil of wire mounted in the horizontal plane was placed around that part of the ruby sample which protruded from the cavity.

III. EXPERIMENTAL RESULTS

A. Distant ENDOR

In this series of experiments we measured the change in χ' and χ'' of the Cr^{3+} paramagnetic system upon application of a radio-frequency field at the nuclear transition frequency of distant aluminum nuclei. These measurements were made directly, without magnetic

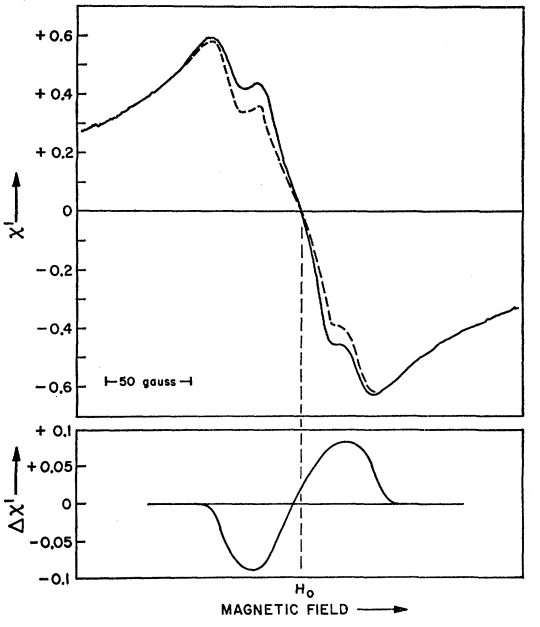

FIG. 3. The effect on the electron paramagnetic χ' when radio frequencies corresponding to Al^{27} nuclear Zeeman frequencies are applied. The top solid curve is the normal χ' curve. The dashed curve is taken point by point and shows that χ' decreases when the rf is applied. The bottom solid curve is the change in χ'; i.e., $\chi'_{\text{rf}}-\chi'_{\text{no rf}}$. The line is broadened and distorted due to the high microwave power being used. Thus the line does not behave as a simple inhomogeneously broadened line. The electronic transition is $S_z=-\frac{1}{2}$ to $S_z=+\frac{1}{2}$. $\theta=0°$.

[11] J. Lambe and R. Ager, Rev. Sci. Instr. **30**, 599 (1959).

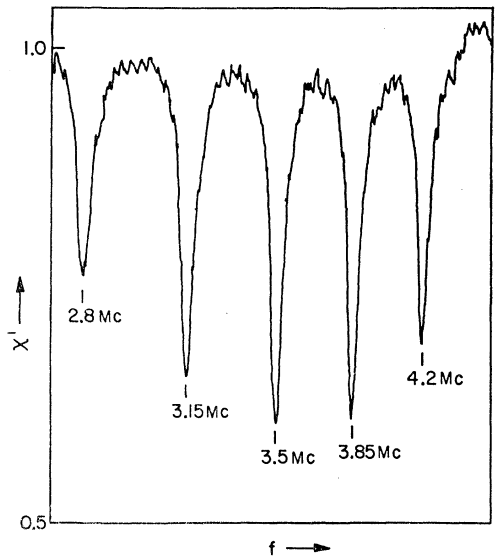

FIG. 4. The effect on the electron paramagnetic χ' as the rf is scanned through the region corresponding to the Al^{27} nuclear Zeeman frequencies.

field modulation, so that the true absorption and dispersion curves and not their derivatives were obtained. In all the experiments to be reported here, the sample was at the temperature of liquid helium with the c axis parallel to the magnetic field. The microwave power level was varied over a range of 0 to 40 db down from 1 mw.

The results for χ' are shown in Fig. 3. When rf corresponding to one of the Al^{27} resonant frequencies is applied to the sample, χ' decreases. This curve was taken point by point, since the aluminum resonant frequency shifts as the static magnetic field is moved across the line. There are five such Al^{27} resonant frequencies, as shown in Fig. 4. The effect vanishes near the center of the resonance line. In order to show the effect, the EPR absorption line must be partially saturated. Within the range of microwave power used in the observation, the effect became more pronounced as the degree of saturation increased.

In Fig. 5 one sees that the effect of applying power at the Al^{27} resonant frequency is to increase χ''. In this case also, the effect vanishes near the center of the resonance line. Both this curve and that of Fig. 3 were taken at a microwave power level 20 db down from 1 mw. The percentage change in χ'' is comparable with that in χ', while in absolute magnitude the χ' signal is about thirty times as great as χ''. If the microwave power is increased further, the percentage change in χ' increases, approaching 50% at 10 db down from 1 mw, while the percentage change in χ'' remains fairly constant.

In order to ensure that the foregoing effects are not due to a shift of the EPR line due to the polarization of the distant nuclei, the following experiment was performed. Microwave power sufficient to produce significant saturation was applied to the sample for a period of approximately 1 min. The power was then quickly reduced to a value well below that required for saturation. After switching to low power, we observed χ' as a function of time and saw no change. The switching operation was completed in less than a second, while distant nuclear polarization is known to relax with a time constant of 10 sec at this temperature. Any shift related to the nuclear polarization should have been observed.

B. Local ENDOR

In these experiments, attention is focused on radio frequencies which flip the spins of Cr^{53} nuclei (10% abundant isotope, $I=\frac{3}{2}$). These frequencies are calculated from the hyperfine coupling constant $A=50$ Mc/sec. The hyperfine levels will have a spacing of approximately 25 Mc/sec for the states $S_z=\pm\frac{1}{2}$, and a spacing of approximately 75 Mc/sec for the states $S_z=\pm\frac{3}{2}$. When these frequencies are applied to the sample, ENDOR effects are observed in χ' and χ'' which are similar in all respects to those observed in the case of distant ENDOR (Figs. 3 and 5). In particular, the recovery time of the dispersion signal after the removal of the local-ENDOR frequency was measured and is shown in Fig. 6. The recovery time, approx 10 sec, is of the same order as the nuclear spin-lattice relaxation time determined by NMR of distant nuclei. In contrast, the electron spin-lattice relaxation time is 0.1 sec.

In addition to the major recovery with a time constant of about 10 sec, there was also a small component

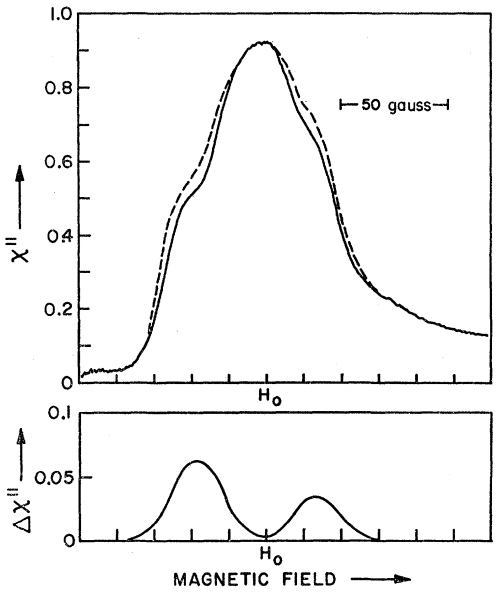

FIG. 5. The effect on the electron paramagnetic χ'' of applying rf corresponding to Al^{27} nuclear Zeeman frequencies. χ'' increases. The top solid curve is taken without rf. The dashed curve, taken point by point, shows the effect of applying rf. The bottom solid curve represents $\chi''_{\text{rf}}-\chi''_{\text{no rf}}$.

which recovered rapidly. The fast effect was only about 1% of the total ENDOR effect and had a time constant of less than a second. This fast effect was not seen in distant ENDOR.

C. NMR Observation of Local ENDOR

The above results indicated that the local ENDOR effect might occur through a coupling of local nuclei to distant nuclei. To clarify this coupling, a double nuclear resonance apparatus was devised. The effect of power at the Cr^{53} resonant frequencies on the NMR of distant Al^{27} nuclei could then be studied.

The experiment was performed by placing one end of a ruby sample in the microwave cavity and winding a NMR coil on that part of the sample which protruded, as shown in Fig. 2. A loop of wire around the sample induced Cr^{53} transitions while the Al^{27} NMR was monitored with a marginal oscillator. Microwave power applied to the EPR enhanced the Al^{27} NMR signal. When power at a radio frequency corresponding to Cr^{53} nuclear transitions was applied, the NMR signal decreased, as shown in Fig. 7. This decrease corresponded to a decrease in the polarization of the Al^{27} nuclei.

This experiment was also carried out in the absence of microwave power. The sensitivity is less, since the initial polarization of the Al^{27} nuclei is only that due to the Boltzmann distribution among the Zeeman levels.

Apparently there exists an effective coupling which permits energy to flow from the Cr^{53} nuclear system into the Al^{27} system. This coupling allows one to observe the hyperfine structure of the Cr^{53} ion in concentrations of 0.01% by monitoring the nuclear magnetic resonance of the abundant Al^{27}.

D. Dilute Ruby and Other Materials

To establish some of the more general aspects of distant ENDOR and local ENDOR, experiments were

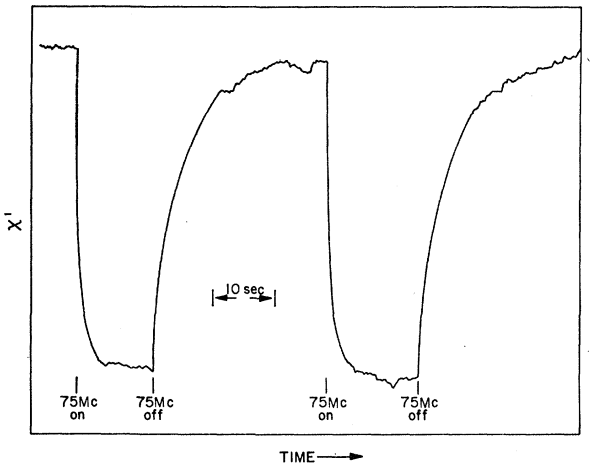

FIG. 6. Response time of the electron paramagnetic χ' when rf corresponding to Cr^{53} nuclear transitions is applied and removed. The recovery time is approximately 10 sec.

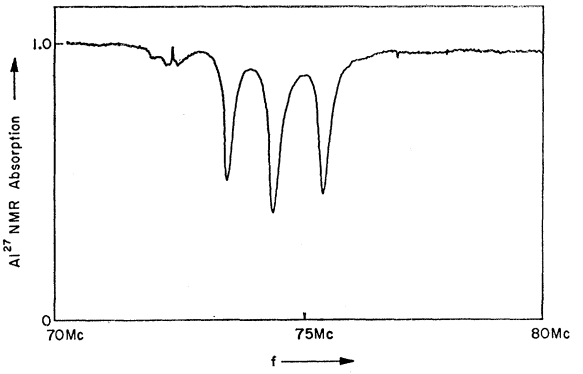

FIG. 7. The effect on the Al^{27} nuclear resonance absorption of introducing Cr^{53} nuclear transitions. The effect is shown here with microwave power also applied, enhancing the Al^{27} nuclear resonance signal by introducing dynamic nuclear polarization. The effect can also be observed without microwave power.

carried out on dilute ruby (Al_2O_3: 0.01% Cr^{3+}), isotope-enriched ruby (>99.9% Cr^{52}), sapphire with Fe^{3+} doping, and chromium-doped "GASH" [$C(NH_2)_3AlSO_4 \cdot 6H_2O$: Cr^{3+}]. In these experiments, magnetic field modulation was used to give increased sensitivity, since the interest was only in observing general effects and the associated recovery times.

The experiments on 0.01% ruby had two objectives. Firstly, the ENDOR time constant was expected to be much longer, since the nuclear spin-lattice relaxation time in 0.01% ruby is about 1 min. Indeed, the ENDOR recovery time was increased to about 1 min.

Secondly, it was hoped that the rapid-response local ENDOR described by Feher might be seen as the result of flipping Al^{27} nuclei which were very close to the chromium ion and had appreciable hyperfine interaction. Such a response had been looked for in 0.1% ruby in vain. The longer time constant of the dominant distant-ENDOR effects made the quest for rapid local-ENDOR effects more hopeful in dilute ruby. A group of ENDOR lines appeared which could indeed be identified with nearby aluminum nuclei. These lines have a much faster response time than distant-ENDOR lines. The time appeared to be less than 1 sec, but no detailed measurements were made. The analysis of this ENDOR spectrum should yield details of the hyperfine coupling of the Al^{27} nuclei to the Cr^{3+} paramagnetic site.

The isotope-enriched ruby showed typical distant-ENDOR effects, indicating that the presence of the magnetically -active Cr^{53} nuclei is not essential to the mechanism.

Experiments were performed on sapphire doped with 0.1% iron, which is in the state Fe^{3+}. Observation of the EPR of the iron ions showed typical distant-ENDOR effects, just as in the case of ruby. The observed Al^{27} nuclear spectrum was, of course, the same as for ruby.

The work on GASH had its primary utility in showing that distant-ENDOR effects are not specific to Al_2O_3. In the case of GASH, the distant nuclei of interest were the protons. When rf power was applied to the distant

proton resonance, large effects were observed in the EPR dispersion signal. These effects were qualitatively the same as those noted for ruby.

IV. NUCLEAR-POLARIZATION MODEL OF DISTANT ENDOR

A description is given of a model spin system which is useful in the analysis of a distant-ENDOR mechanism wherein the applied rf simply removes a previously established dynamic nuclear polarization. This model system shows the qualitative behavior which was observed in the distant-ENDOR experiments on ruby. Although the magnitudes and linewidths used correspond to an idealized ruby line, the detailed behavior of a particular material is ignored. The analysis should apply rather generally to depolarization-induced changes in inhomogeneously-broadened resonance lines.

The model spin system consists of a population of electron spins interacting with distant spin-$\frac{1}{2}$ nuclei through weak "forbidden" transitions in which both spins flip. Because of a local field distribution $h(\omega'-\omega_0)$, the EPR line is inhomogeneously broadened about its center ω_0 with linewidth $1/T_2^*$. The line shape is normalized with

$$\int_0^\infty h(\omega'-\omega_0)d\omega'=1. \quad (1)$$

The nuclear Zeeman splitting Δ is assumed small compared to $1/T_2^*$, while the natural linewidth $1/T_2$ (the width of a spin packet) is assumed small compared to Δ. The natural line-shape function $g(\omega-\omega')$ satisfies the normalization condition

$$\int_0^\infty g(\omega-\omega')d\omega'=1. \quad (2)$$

The steady-state solution of the coupled equations of motion of the electron spins and the nuclear spins will be sought. This solution will give the expected value of the dynamic nuclear polarization.[7-9] The change in the electron spin population upon removal of the dynamic nuclear polarization (through the application of rf at the nuclear transition frequency) may then be evaluated.

The remainder of the analysis rests upon the work of Portis on inhomogeneous broadening.[12] The derived expression for the spin population difference is used in the integrals of Portis' paper. The susceptibility is then evaluated as a function of nuclear polarization, and the response of the EPR signal to the applied rf power is found.

Population Dynamics. If microwave power is applied at a frequency ω, the allowed electron-spin transitions (no change in distant nuclei) are stimulated in the population $h(\omega'-\omega_0)$ with a shape factor $g(\omega-\omega')$. In addition, the "forbidden" double spin-flip transitions, where a distant nucleus flips its spin simultaneously with an electron, will result in additional power absorption with the same shape, a reduced probability, and centered at $\omega\pm\Delta$. The shape factors will be represented by $g'(\omega\pm\Delta-\omega')$ with a normalization g' (the relative strength of forbidden and allowed transitions):

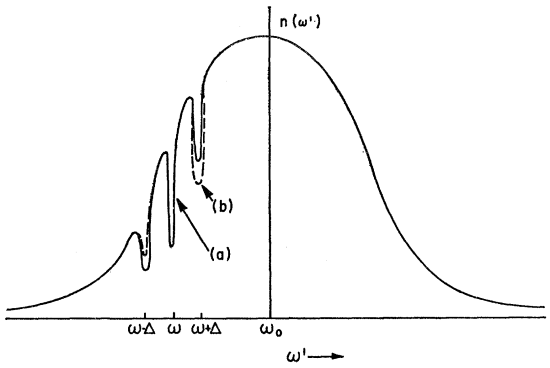

FIG. 8. Electron-spin population changes upon application of the ENDOR frequencies.

$$\int^\infty g'(\omega\pm\Delta-\omega')d\omega'=g'. \quad (3)$$

The following notation will be used:

$N(\omega')=h(\omega'-\omega_0)$: the distribution function of electrons in local fields. $N(\omega')d\omega'$ gives the fraction of electrons which are in a local field such that their resonance lies between ω' and $\omega'+d\omega'$.

$N^-(\omega')$: that part of $N(\omega')$ which has spin down.

$N^+(\omega')$: that part of $N(\omega')$ which has spin up.

$n(\omega')=N^-(\omega')-N^+(\omega')$: the difference in electron spin populations.

And for the distant nuclear spins:

M^-: the fraction of nuclei with spin down.

M^+: the fraction of nuclei with spin up.

$m=M^--M^+$: the difference in nuclear-spin populations.

It follows from these definitions that

$$[M^-N^-(\omega')-M^+N^+(\omega')]=\tfrac{1}{2}[n(\omega')+mN(\omega')] \quad (4)$$

and

$$[M^+N^-(\omega')-M^-N^+(\omega')]=\tfrac{1}{2}[n(\omega')-mN(\omega')] \quad (5)$$

in the transport equations below. Equilibrium values of m and $n(\omega')$ in the absence of fields are represented as m_0 and $n_0(\omega')$.

The coupled equations for a steady state[12] will be written in a relaxation-time approximation, with T_1 the spin-lattice relaxation time for electrons and T_N the nuclear spin-lattice relaxation time:

[12] A. M. Portis, Phys. Rev. **91**, 1071 (1953).

$$[n_0(\omega')-n(\omega')]/T_1=\tfrac{1}{4}\pi\gamma^2H_1^2\{g(\omega-\omega')[N^-(\omega')-N^+(\omega')]$$
$$+g'(\omega+\Delta-\omega')[M^+N^-(\omega')-M^-N^+(\omega')]+g'(\omega-\Delta-\omega')[M^-N^-(\omega')-M^+N^+(\omega')]\}, \quad (6)$$

$$(m_0-m)/T_N=\tfrac{1}{4}\pi\gamma^2H_1^2\Big\{\int g'(\omega-\Delta-\omega')[M^-N^-(\omega')-M^+N^+(\omega')]d\omega'$$
$$-\int g'(\omega+\Delta-\omega')[M^+N^-(\omega')-M^-N^+(\omega')]d\omega'\Big\}, \quad (7)$$

where γ is the electron gyromagnetic ratio and H_1 is the magnitude of the microwave field.

Using Eqs. (4) and (5), and the definition of the parameter

$$S=(\tfrac{1}{2}\gamma H_1)^2T_1T_2, \quad (8)$$

it is possible to rewrite Eq. (6) in the following useful form:

$$n(\omega')=\frac{n_0(\omega')+(\pi S/2T_2)N(\omega')[g'(\omega+\Delta-\omega')-g'(\omega-\Delta-\omega')]m}{1+(\pi S/2T_2)[2g(\omega-\omega')+g'(\omega+\Delta-\omega')+g'(\omega-\Delta-\omega')]}. \quad (9)$$

The steady-state nuclear-spin solution, given by

$$m=\frac{m_0+(T_NS/2T_1T_2)\int n(\omega')[g'(\omega+\Delta-\omega')-g'(\omega-\Delta-\omega')]d\omega'}{1+(T_NS/2T_1T_2)\int N(\omega')[g'(\omega+\Delta-\omega')+g'(\omega-\Delta-\omega')]d\omega'} \quad (10)$$

may be approximated by

$$\frac{m}{m_0}=\frac{1+(2T_N/T_1T_2)[\frac{1}{2}g'S/(1+\frac{1}{2}g'S)]h(\omega-\omega_0)[1+(4/\pi)(T_2^*)^2\omega(\omega_0-\omega)]}{1+(2T_N/T_1T_2)[\frac{1}{2}g'S/(1+\frac{1}{2}g'S)]h(\omega-\omega_0)(1+\frac{1}{4}g'S)}, \quad (11)$$

where advantage has been taken of the relative size of $1/T_2^*$, Δ, and $1/T_2$. The important feature of this solution is that, for all the line $h(\omega-\omega_0)$ except the extreme wings and the immediate vicinity of the peak ω_0, m is proportional to $(\omega_0-\omega)$. Thus the nuclear-spin temperature is positive for $\omega<\omega_0$, and is negative on the high-frequency side of the peak. So far this is simply a calculation of the Abragam dynamic nuclear polarization[7] set up through the action of normally forbidden transitions.

The application of rf power sufficient to saturate the nuclear resonance then changes m from the steady-state value given by (11) to a value $m=0$. The second term in the numerator of (9) then vanishes, effectively changing the line shape. Figure 8 shows $n(\omega')$ for $\omega<\omega_0$, with and without applied rf.

The following subsection will be anticipated here in order to make the qualitative observation that the change in electron-spin population upon application of an ENDOR signal deepens one of the "side-band" holes, makes the other one shallower. The resulting two changes in absorption tend to cancel, while the changes in dispersion reinforce. Consequently, it is to be expected that the ENDOR mechanism described here will show more sensitively in dispersion than in absorption.

Spin Susceptibility. Having derived an expression (9) for the difference in electron-spin population as a function of nuclear-spin polarization, one may now calculate the real and imaginary parts of the spin susceptibility, using the integrals of Portis' paper [Eqs. (17) and (18) of reference 12].

In analogy to Portis' Eq. (19), the following expression is found for absorption:

$$\chi''(\omega)=\tfrac{1}{2}\chi_0\omega_0h(\omega-\omega_0)\Big\{\int_0^\infty\frac{\pi g(\omega-\omega')d\omega'}{1+(\pi S/T_2)g(\omega-\omega')}$$
$$+\text{constant term}$$
$$-m(\omega_0-\omega)\ [\text{positive definite term}]\Big\}. \quad (12)$$

The change in absorption upon application of the ENDOR signal (change in χ'' when m becomes zero) will be small. It will always be an increase, however.

In calculating the dispersion, a double integration leads to products of natural line shapes about the same center, so that contributions of the forbidden transitions will be significantly larger in dispersion than in absorption. In analogy to Portis' Eq. (20), the dispersion may be approximated by

$$\chi'(\omega)=\tfrac{1}{2}\chi_0\Big\{\int_0^\infty\frac{2\omega'^2h(\omega'-\omega_0)d\omega'}{\omega'^2-\omega^2}$$
$$+\left(\frac{m}{m_0}\right)\frac{\frac{1}{2}g'S}{(1-\frac{1}{2}g'S)}\left(\frac{2\pi}{T_2}\right)h(\omega-\omega_0)\Big\}. \quad (13)$$

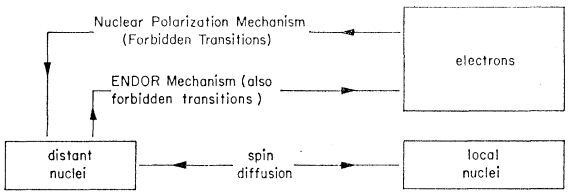

FIG. 9. A schematic representation of the nuclear-polarization mechanism. The important interactions are apparently spin diffusion, which ties the local nuclei to the distant nuclei, and forbidden transitions involving distant nuclei, which produce both dynamic nuclear polarization and the ENDOR effects.

It was previously noted that $m>0$ for $\omega<\omega_0$, and $m<0$ for $\omega>\omega_0$ (except for the extreme wing and the vicinity of the peak). From (13), consequently, it may be seen that the term proportional to m will be of the same sign as the first term of χ' [except very near $\omega=\omega_0$ and for $(\omega-\omega_0)\gg 1/T_2{}^*$]. Thus the application of an ENDOR signal will decrease the magnitude of the dispersion signal, since the term proportional to m will vanish upon the application of rf.

This "nuclear-polarization" model of distant ENDOR, based on the removal of dynamic nuclear polarization by applied rf, then gives qualitative agreement as to the sign of the changes in χ' and χ'', but predicts a small absorption-ENDOR effect in the case of narrow spin packets.

V. DISCUSSION

A. Nuclear-Polarization Model of ENDOR

The similarities between the response of the EPR signal to the Al^{27} and the Cr^{53} NMR frequencies is striking. In both cases χ' decreases significantly, χ'' increases moderately. Both the local-ENDOR effect (Cr^{53} nuclei) and the distant-ENDOR effect (Al^{27} nuclei) recover with the spin-lattice relaxation time of the aluminum nuclei. The double-nuclear resonance observations, which show that the distant Al^{27} nuclei depolarize upon the application of rf to induce Cr^{53} NMR transitions, confirm the existence of an effective coupling (apparently spin diffusion) between these two nuclear populations. All indications are that the mechanisms of local and distant ENDOR in ruby are the same.

The question to be answered is then: What is the ENDOR mechanism which comes into play when rf is applied to either of these two nuclear populations? Feher explained his results[4] by suggesting that unsaturated electron-spin packets were being shifted by the rf transitions of nuclei. In ruby, the distant aluminums do not contribute appreciably to the EPR linewidth, and so saturating distant aluminum nuclei does not shift spin packets even an appreciable fraction of their width. This cannot be the explanation. Saturating Cr^{53} nuclei does shift spin packets; in fact, shifts them from one resolved hyperfine level to another. However, the experiments with isotope-enriched ruby, in the virtual absence of magnetically active chromium nuclei, produced identical distant-ENDOR behavior. So the presence of Cr^{53} nuclei is not essential to the mechanism.

The most probable mechanism intrinsically involves forbidden transitions and dynamic nuclear polarization by the Abragam scheme[7] (Fig. 9). In brief, this model predicts the changes in electron-spin population-difference illustrated in Fig. 8. With the rf power applied, there are equal numbers of nuclei in the two spin states. The saturation of the NMR thus assures equal nuclear populations taking part in the two types of forbidden transitions (S^+I^+ and S^+I^- transitions). The resulting "line shape" is the dashed line of Fig. 8. [It should be stressed that this is not the shape of any line to be found in experimental data, but is the shape of the electron-spin population difference $n(\omega')$ for a given applied frequency ω].

Without the rf power equalizing nuclear-spin populations, a dynamic nuclear polarization is set up which satisfies the principle of detailed balance for the nuclear spins with respect to the S^+I^+ and S^+I^- processes. The result (for $\omega<\omega_0$) will be an increase in the number of nuclear spins which are candidates for the S^+I^+ processes and a decrease in those which are candidates for the S^+I^- processes. The former processes then go more strongly, the latter more weakly. The electron-spin population difference in the steady state becomes that depicted by the solid line of Fig. 8.

In order to find the magnitude of the fractional changes in the real and imaginary parts of the spin susceptibility upon application of the ENDOR signal, a set of numerical values may be assumed which approximately correspond to the ruby experiment. From the linewidth, $1/T_2{}^*=20$ Mc/sec for $\omega_0=10^4$ Mc/sec. From saturation measurements as a function of H_1, the spin-packet width may be approximately determined. This somewhat rough determination gives $1/T_2=0.2$ Mc/sec. The nuclear Zeeman splitting is about 3.0 Mc/sec, $T_1=0.1$ sec, and $T_N=10$ sec. The only undetermined parameter is g', and a fair fit seems to occur for $g'\approx 0.01$. Using these numbers in Eqs. (11), (12), and (13), the enhancement of nuclear polarization and the fractional change in the real and imaginary parts of the spin susceptibility may be calculated and compared with experiment (Table I).

The numerical results of the nuclear-polarization

TABLE I. A comparison of experimental data with predictions of the nuclear-polarization model. Values of the dynamic nuclear polarization enhancement (m/m_0) and fractional changes in the real and imaginary parts of the spin susceptibility are tabulated, under two different saturation conditions.

	$S=20$		$S=200$	
	Theory	Experiment	Theory	Experiment
m/m_0	25	45[a]	100	75[a]
$\Delta\chi'/\chi'$	−0.06	−0.15	−0.55	−0.50
$\Delta\chi''/\chi''$	0.0003	0.07	0.02	0.10

[a] See reference 9.

model correspond qualitatively with experiment, and give semiquantitative agreement to measured nuclear polarizations and dispersion signal changes. The observed change in absorption signal is larger than the predicted value, however. If the spin-packet width $1/T_2$ used in the calculations is correct, the change in absorption signal may have another origin. One possibility would be enhanced spectral spin diffusion.[13] If the application of rf increases the rate of spin diffusion within the line, then effectively the value of T_2 is decreased, the packet width increases, and the saturation parameter S is reduced. This would lead to an increase in χ'' as observed.

It is also possible that in 0.1% ruby, the spin packets are ill-defined. In the presence of a dense population of paramagnetic centers, T_2 may be considerably shortened and $1/T_2$ may be comparable to Δ. The approximations used in obtaining Eqs. (11), (12), and (13) would then be invalid. The absorption effects would be much larger than calculated. The treatment remains qualitatively correct even in the absence of well-defined spin packets: the absorption increases and the dispersion decreases upon removal of the dynamic nuclear polarization. It will be recalled that fast-response local-aluminum-ENDOR effects, which were observed in dilute ruby, could not be seen in 0.1% ruby. This may be taken as corroborating evidence that spin packets are not well defined in 0.1% ruby.

If distant ENDOR is taken to be the dynamic result of changes in distant-nuclear polarization, the response and recovery times for ENDOR effects might easily be equal to the spin-lattice relaxation time of the nuclei. It is generally accepted that relatively short nuclear relaxation times such as those of ruby are due to relaxation through paramagnetic impurities.[14,15] The characteristic time for relaxation of nuclei through the paramagnetic spins should also be the characteristic time for the paramagnetic spin system to respond to changes in the distant-nuclear polarization, through the same interaction.

There is another interesting point of qualitative agreement. The steady-state solution for m given by (11) is nonzero for $\omega=\omega_0$, so a small ENDOR effect is predicted at the center of the line. The value of ω for which (11) predicts $m=0$ is somewhat greater than ω_0; consequently there should be a point of "zero ENDOR effect" at fields somewhat below H_0 in the experimental configuration. This asymmetry is observed experimentally (Figs. 3 and 5).

To sum up, distant and local ENDOR in ruby could both be responses to depolarization of distant nuclei. The analysis of Sec. IV would apply to both cases, perhaps with a generalization needed to broad spin packets. The only difference between local and distant ENDOR in ruby would be the technique of removing the dynamic nuclear polarization. In distant ENDOR, depolarization is produced directly by applying rf at the distant-nuclear Zeeman frequencies. In local ENDOR, depolarization results from the interaction of Cr^{53} nuclei with the distant Al^{27} nuclei, the depolarization of the Cr^{53} inducing a depolarization of the Al^{27}.

B. Packet-Shifting ENDOR Mechanisms

In the preceding sections, we have emphasized the process of nuclear depolarization as a basis for ENDOR effects. We have shown that a local ENDOR effect can operate through a depolarizing action on distant nuclei.

It is to be emphasized that the local ENDOR mechanism proposed here by no means excludes the packet-shifting mechanism proposed by Feher. Indeed, in dilute ruby (0.01% Cr) both mechanisms are operative. It was previously noted that the shifting of spin packets increased the absorptive part of the spin susceptibility by introducing new spin packets to be saturated. At the same time, this shifting tends to move the previously-burned "hole" (the saturated spin packets) preferentially towards the center of the inhomogeneous line. This reduces the dispersive spin susceptibility. Thus both the spin-packet model and the depolarization model predict an increase in χ'', a decrease in χ'.

The major experimentally observed difference between the two types of local ENDOR is in the recovery time of the ENDOR effect. Depolarization local ENDOR has a time characterized by the distant nuclear T_1; packet-shifting local ENDOR has a time characterized by the electron T_1.

VI. CONCLUSION

A. Mechanism

A possible mechanism of distant-ENDOR behavior has been discussed in this paper. It involves the removal of a dynamic nuclear polarization and predicts the correct qualitative behavior as well as the observed response time. A sure choice cannot be made on the basis of available experiments, but several features favor this nuclear-polarization mechanism.

The model relies upon a close connection (presumably through spin diffusion) between the local and distant nuclei. Power applied to one nuclear resonance then influences all nuclear populations, local and distant. The long time constant for local ENDOR is explained by the "reservoir" action of the distant nuclei: The distant-nuclear population must readjust before the local-nuclear population can reach a new steady-state condition.

The important interactions are sketched in Fig. 9. The forbidden transitions with distant nuclei set up a dynamic nuclear polarization. Application of rf to either distant or local nuclei removes this polarization, thus causing a dynamical change in the electron-spin population difference. This affects the dispersion greatly, the absorption to a smaller extent.

[13] A. M. Portis, Phys. Rev. **104**, 584 (1956).
[14] N. Bloembergen, Physica **15**, 386 (1949).
[15] W. E. Blumberg, Phys. Rev. **119**, 79 (1960).

It must be emphasized that local ENDOR effects can also occur via the spin-packet shifting mechanism proposed by Feher. The depolarization mechanism proposed here gives local ENDOR with recovery times comparable to nuclear T_1. The packet-shifting local ENDOR has recovery times comparable to electron T_1. Both of these mechanisms can occur in a given material, as was seen in dilute (0.01% Cr) ruby.

B. Techniques

Operationally, two interesting aspects of double resonance work appear in this paper. The first is simply the existence of a distant-ENDOR effect. The second is the applicability of double-nuclear resonance to dilute nuclear populations.

Since it is believed that distant nuclear spins in many materials relax through interaction with paramagnetic impurities, it is to be expected that the appropriate coupling exists in many materials to allow the observation of EPR responses to the depolarization of distant nuclei. The generality of the technique will be limited by the operational problem of the distant-nuclear spin-lattice relaxation time. If this is long, it will be experimentally difficult to observe distant-ENDOR responses. The distant-ENDOR technique should be generally applicable in the presence of dense paramagnetic centers, however.

A double-nuclear resonance experiment was performed wherein the application of rf to a dilute population of one nuclear species affected the existing Boltzmann polarization of the much denser "detector" nuclei. This technique may be quite generally applicable. In the presence of dense paramagnetic centers, a "triple resonance" technique allows an enhancement of the sensitivity of nuclear-nuclear double resonance. Microwave power is applied to one side of an inhomogeneous EPR line belonging to the paramagnetic impurities, giving the detector-nuclei a dynamic nuclear polarization larger than the usual Boltzmann polarization. They then become more sensitive in their response to changes in the second nuclear population.

ACKNOWLEDGMENTS

We wish to thank N. Bloembergen, G. Feher, C. Kikuchi, and A. Overhauser for many stimulating and helpful discussions.